

# PARAMETRIC ANALYSIS ON ANNUAL VARIATION OF SURFACE HEAT EXCHANGE AND THERMAL STRUCTURE IN LAKES

By

K. Michioku

Kobe University, Rokkodai, Nada, Kobe, Japan

and

K. Kadoyu

Ministry of Construction

## SYNOPSIS

An analytical work is performed to examine the effects of lake depth and meteorological factors upon thermal regimes in lakes. Stratified temperature field is analytically described by means of a one-dimensional mixed-layer model. Surface heat flux is expressed by a simplified heat exchange relationship, where an equilibrium temperature with a sinuous function of time is introduced to describe the seasonal variation of meteorological conditions. In this case, we need not specify time-dependent functional form of surface heat flux, which is given as a solution of the analysis. Vertical mixing process is analytically described by the entrainment laws which are proposed in the author's previous experimental study. Computed seasonal development of temperature field and surface heat exchanges are in satisfactory agreement with field data. Normalization of basic equations leads to two governing parameters, with which a parametric analysis is performed. Based on the analysis, lakes are classified into three categories; (a) stratified lakes (or thermo-dynamically deep lakes), (b) moderately-mixed lakes and (c) well-mixed lakes (or thermo-dynamically shallow lakes).

## INTRODUCTION

The thermal cycle in lakes is strongly affected by meteorological conditions as well as by lakes' dimensions such as water depth. This is definitely a different point from situations in oceans or atmospheric boundary layers which are semi-infinite systems bounded solely by the air-water interface or ground surfaces. In lakes, the bottom boundary inhibits thermal stratification development, which modifies temperature profiles and surface heat exchange. For instance, in shallow lakes, turbulent patches generated by wind shear and/or by natural convection are easily transported to the lake bottom, which promotes full scale mixing and then produces a homogeneous temperature field; on the other hand, in deep lakes, penetration of turbulence kinetic energy is confined within a surface layer of finite thickness below which a stable stratification develops. Hydrodynamic differences between shallow and deep lakes can be found not only in thermal structure but also in surface heat exchange process; total amount of surface heat exchange throughout a year in a shallow lake is generally less than that in a large lake because of their heat capacity difference, even if both are under the same meteorological conditions.

In this paper, we examine how lake water depth, wind intensity and thermo-dynamic factors of meteorology affect seasonal variation of water temperature, stratification and destratification processes, heat transfer across the air-water interface and so on. Main factors considered here are

(a) meteorological conditions governing surface heat flux, (b) mechanical stirring due to wind shear stress and (c) depth of lakes. The focus is on seasonal temperature variation whose time scale is longer than that of hourly or daily variation. In this case, heat and mass transfer in the vertical direction plays more dominant roles on lake thermo-dynamics than the horizontal component. The system is considered to be vertically one-dimensional. An integral mixed-layer model is employed to describe thermal processes in lakes. Vertical mixing is formulated by means of entrainment relationships. Heat exchange across the water surface is given by a linearized heat exchange relationship in which heat flux is in proportion to temperature deviation of surface water from an equilibrium temperature. Temperature analysis is performed under a fairly simplified situation, i.e. seasonal variation of an equilibrium temperature is approximated to be single harmonic and wind stress imposed on water surface is assumed to be constant. Basic equations are normalized with characteristic scales to get dimensionless parameters. Performing a parametric analysis, we found functional relationships between the thermal regimes in lakes and the two parameters defined by lake depth, wind shear stress and heat flux magnitude. From a thermo-dynamic point of view, lakes are classified into three categories, i.e., (a) stratified lakes (or thermo-dynamically deep lakes), (b) moderately mixed lakes and (c) well mixed lakes (or thermo-dynamically shallow lakes), respectively.

#### HEAT EXCHANGE AT THE WATER SURFACE

Heat flux across the water surface is a function of meteorological conditions and water surface temperature. Although the functional relationship is more or less non-linear and complicated, heat transfer process is approximated by the following bulk formula

$$Q_N = -K(T_e - T_s) \quad (1)$$

where,  $Q_N$  (cal/cm<sup>2</sup>/day) : surface heat flux,  $T_e$  : equilibrium temperature, and  $T_s$  : surface water temperature. Eq. 1, where all of meteorological factors governing heat transfer processes are included in  $T_e$ , is a linearized heat flux relationship developed by Tetzlaff (1979) (1). The heat exchange coefficient  $K$  is given by

$$K = 4\epsilon\sigma\Delta^3 + h + s\beta \quad (2)$$

where,  $\epsilon$  : emissivity of the water surface (=0.97),  $\sigma$  : Stephan-Boltzmann's coefficient ( $11.7 \times 10^{-8}$  (cal/cm<sup>2</sup>day°C<sup>4</sup>)),  $\Delta = 273$  (°C),  $h$ ,  $s$  : exchange coefficients for sensitive and latent heat transfer, respectively and  $\beta = de/dT$  : gradient of "saturation vapor pressure" curve. Detail procedures to obtain Eqs. 1 and 2 may be referred to (1).

To obtain higher resolution in water temperature prediction, meteorological data in-situ should be used. The purpose of the present study is, however, not to make a case study but to obtain general features of lake thermo-dynamics. Therefore,  $K$  in Eq. 1 will be treated to be constant to make the analysis simple. Numerical values for  $K$  will be discussed later.

#### OUTLINE OF TEMPERATURE ANALYSIS

Three Phases of Thermo-dynamic Process in Lakes and Their Entrainment Relationships (2)

It is shown that annual development of lake thermal structure is classified into the three phases in our previous paper (2), which are briefly summarized as follows.

(I) The first phase of heating season : "H<sub>1</sub>"

In earlier heating season, mechanical turbulence produced by wind shear seldom penetrates into thermocline interface, because, in this stage, the thermocline is deep. Meanwhile, heat flux supplies stable buoyancy which increases dynamic stability of density field. In such a situation, the mixed-layer depth  $h_m$  is determined from the following relationship

$$C_w u_*^3 - C_b u_b^3 = 0 \quad (3)$$

where,  $C_w, C_b$  : empirical coefficients denoting efficiency of wind-induced mechanical turbulence and heating buoyancy flux on mixing, respectively,  $u_*$  : friction velocity of wind shear. A velocity scale for buoyancy flux due to heating,  $u_b$ , is defined by  $u_b = (-\alpha g F(t) h_m)^{1/3}$ , where  $\alpha$  : a thermal expansion coefficient,  $g$  : gravity acceleration,  $F(t)$  ( $^{\circ}\text{C cm/sec}$ ) =  $Q_N/\rho c$  : heat flux per unit area divided by density,  $\rho$ , and specific heat of water,  $c$ . Note that a negative value of  $F(t)$  means that heat is transferred from atmosphere to water body and *vice versa*.

Eq. 3 gives a solution of thermocline depth  $h_m$ , for which mechanical turbulence kinetic energy,  $C_w u_*^3$ , is just in balance with stabilizing effect of buoyancy flux,  $C_b u_b^3$ . With increasing heat flux magnitude  $|F(t)|$ , the mixed-layer gradually becomes thinner.

(II) The second phase of heating season : H<sub>2</sub>

As the mixed-layer thickness  $h_m$  decreases, relative contribution of buoyancy flux,  $u_b^3$ , to stratification process becomes less important. Instead, the wind-induced mechanical turbulence,  $u_*^3$ , becomes more dominant on mixed-layer development. After the mixed-layer thickness reaches a certain minimum value  $h_{ms}$ , the two terms of Eq. 3 no longer remain in balance. In this stage, the mechanical stirring overcomes the stabilizing buoyancy flux, which promotes weak vertical mixing. According to the author's previous experimental work (3), the mixing velocity or the thermocline deepening rate,  $(dh_m/dt)$ , was found to be

$$\frac{dh_m}{dt} = C_w \frac{u_*^3}{\varepsilon g h_m} - C_b \frac{u_b^3}{\varepsilon g h_m} \quad (4)$$

where,  $\varepsilon = \alpha \Delta T$  : specific density difference across the thermocline and  $\Delta T$  : temperature jump there.

## (III) Cooling season : C

In the cooling season, heat flux  $F(t)$  becomes positive, which contributes to turbulence energy production through thermal convection. In this case, the vertical mixing is induced by combined action of mechanical and thermal stirring. In our experimental work (4), it was found that the mixing rate may be described by

$$\frac{dh_m}{dt} = C_w \frac{u_*^3}{\varepsilon g h_m} + C_f \frac{u_f^3}{\varepsilon g h_m} \quad (5)$$

where,  $u_f = (\alpha g F(t) h_m)^{1/3}$  : convection velocity,  $C_f$  : an empirical coefficient measuring efficiency of natural convection on vertical mixing.

The coefficients in Eqs. 3 to 5 were determined as follows (2)

$$C_w = 11.0, C_f = 0.45, C_b = 0.356 \quad (6)$$

Coupling the entrainment relationships given by Eqs. 3 to 5 with a heat conservation equation given later, time development behaviors of thermal structure can be analyzed.

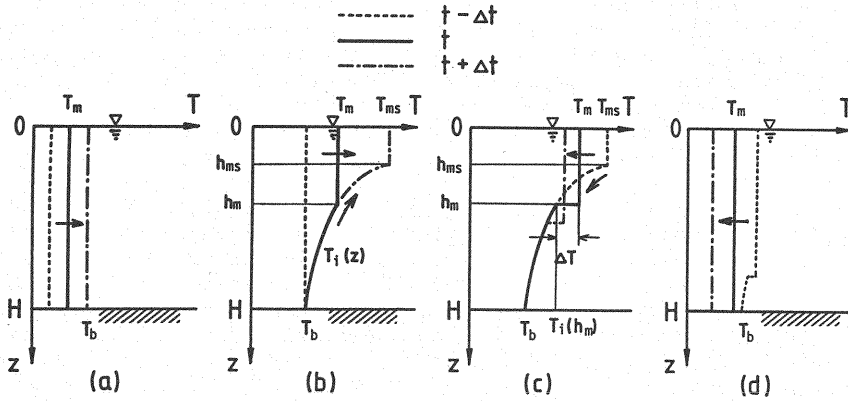


Fig. 1 Schematic of temperature profiles in the present model  
 (a) Initial stage of heating season  
 (b) Formation of stratified structure  
 (c) Vertical mixing and destratification processes  
 (d) Uniformly overturned regime

#### Mixed-Layer Model and Its Heat Conservation

Temperature analysis in the present work is based on an integral mixed-layer model which was originally developed by Kraus & Turner (5). However, this can not be applied directly to the present system, since it is applicable only to infinitely deep bodies such as oceans and atmosphere. The original model should then be modified so that it could be applied to a finite depth lake system. A schematic concept of modified model is shown in Fig. 1. The analytical procedure is as follows.

In the beginning, temperature is considered to be uniformly distributed. Water temperature is defined as the deviation from the initial temperature. Thus, the initial temperature is set to zero in the analysis.

In the earlier heating period, heating is so weak that temperature field is uniformly mixed by wind-induced disturbance. In this stage, the mixed-layer thickness  $h_{me}$  given by Eq. 3 is larger than the total lake depth  $H$ , i.e.  $h_{me} = C_w u_*^3 / \{-C_b agF(t)\} \geq H$ . The corresponding water temperature,  $T_m$ , can be easily computed from the heat conservation relationship,  $dT_m/dt = -F(t)/H$ .  $T_m$  monotonically increases until  $h_{me}$  becoming smaller than  $H$ . The water temperature corresponding to the stage of  $h_{me} = H$  is defined as  $T_b$  (see Fig. 1(a)).

In the second stage, temperature field begins to stratify and to develop a two-layer system. This is composed of a uniformly mixed-layer in the surface region and a continuously stratified layer in the deeper region. Solutions for  $h_m$  and  $T_m$  are obtained by using Eq. 3 and the following heat conservation equation.

$$\int_0^t -F(t) dt = T_m(t) \cdot h_m(t) + \int_{h_m}^H T_i(z) dz = S \quad (7)$$

where,  $S$  : heat storage or heat content of water column with unit horizontal area. Temperature profile in the deep region,  $T_i(z)$ , is assumed to have a permanent form which is equivalent to the functional relationship between  $z = h_m(t)$  and  $T_i(z) = T_m(t)$ , where  $h_m(t)$  and  $T_m(t)$  are a set of solutions for the period of  $H$ , and  $t$  is treated to be a dummy variable between them. In other words, the profile of  $T_i(z)$  is equivalent to a trajectory of the mixed-layer bottom boundary during the heating process in the  $(T, z)$  plane. Fluid at  $z$  in the deep region is considered to keep its temperature  $T_i(z)$  until it would be

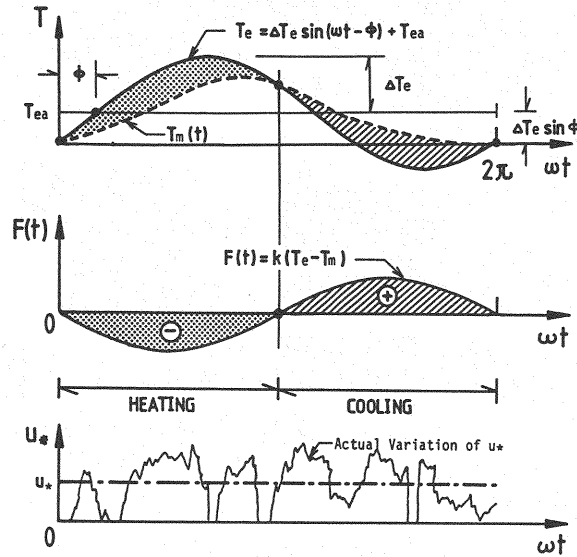


Fig. 2 Schematic diagram for annual variation of heat flux,  $F(t)$ , equilibrium temperature,  $T_e$ , and mixed-layer temperature,  $T_m$

mixed again due to entrainment. The functional form of  $T_i(z)$  is given as follows (2).

$$T_i(z) = T_m(h_m^{-1}(z)) \quad (8)$$

Due to detraining process, the mixed-layer thickness decreases and surface temperature increases until  $h_m$  reaches the minimum value  $h_{ms}$  (see Fig. 1(b)).

The thermal regime then turns to  $H_2$ ; the thermocline begins to deepen due to vertical mixing (Fig. 1(c)). The mixing rate for the period of  $H_2$  and  $C$  are computed from Eqs. 4 and 5, respectively. Solutions for these two regimes are obtained from Eq. 4, Eq. 5 and heat conservation relationship Eq. 7.

Finally, the mixed-layer deepens to the bottom and the system is completely overturned (see Fig. 1(d)). Computation of water temperature in this case is exactly the same as that of Fig. 1(a).

#### External Conditions

External factors imposed on water surface are meteorological conditions such as atmospheric temperature, solar radiation, air humidity, cloud mass, etc. and wind stress. These are given as follows.

It is assumed that seasonal variation of meteorological factors could be described in terms of an equilibrium temperature whose time dependency is sinusoidal as

$$T_e = \Delta T_e \sin(\omega t - \phi) + T_{ea} \quad (9)$$

where,  $\Delta T_e$  : annual amplitude of  $T_e$ ,  $\omega = 2\pi/365$  ( $\text{day}^{-1}$ ) : angular frequency,  $t$  : time,  $\phi$  : phase lag and  $T_{ea}$  : annual average of  $T_e$ .

Replacing surface temperature  $T_s$  in Eq. 1 by the mixed-layer temperature  $T_m$ , heat flux is written as follows.

$$F(t) = Q_N/\rho c = -k(T_e - T_m) \quad (10)$$

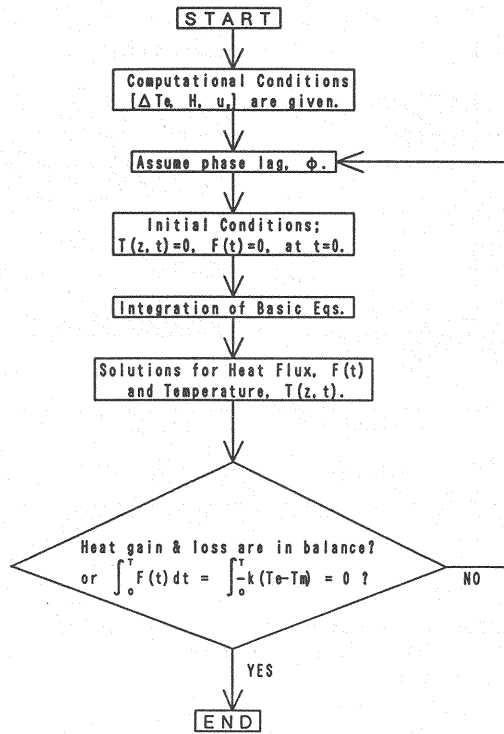


Fig. 3 Computation flow chart in the analysis

where,  $k=K/\rho c$  : a newly defined heat exchange coefficient.

Time dependency of  $F(t)$ ,  $T_e$  and  $T_m$  are schematically shown in Fig. 2.

The other external component, i.e. the wind stress, is not periodical and its time variation is irregular as well as intermittent. To simplify the analysis, however, a constant wind shear velocity,  $u_s$ , is assumed, which may be equivalent to the annual average of mechanical stirring (schematically shown in a chain line in Fig. 2).

Once a set of  $\Delta T_e$  and  $u_s$  are given, seasonal variation of thermal structure could be analyzed. The phase lag  $\phi$  in Eq. 9 is iteratively determined so that annual integration of heat gain and loss become zero, i.e.,

$$\int_0^T F(t) dt = 0 \quad (11)$$

where, the origin of time coordinate,  $t=0$ , is taken so that  $F(t=0)=0$  or  $T_e=T_m=0$  at  $t=0$ . For given  $\phi$  and  $\Delta T_e$ , the average equilibrium temperature  $T_{e,s}$  which satisfies Eqs. 11 is determined to be  $T_{e,s} = \Delta T_e \sin(\phi)$ .

A set of solutions for  $T(z, t)$ ,  $F(t)$  and  $\phi$  are solved according to the flow chart shown in Fig. 3.

Neither ice formation nor inverse temperature stratification below  $4^\circ\text{C}$  is considered in this analysis.

#### NORMALIZATION OF BASIC EQUATIONS TO OBTAIN GOVERNING PARAMETERS

##### Normalization of Basic Equations

In order to perform a parametric analysis, three independent variables,

$\Delta T_e$ ,  $u_*$  and  $1/\omega$ , are chosen as scaling factors, which express the thermal meteorological factors, the wind-induced stirring and time, respectively. Performing a dimensional analysis based on the entrainment relationships, Eqs. 3 to 5 and the heat conservation equation, Eq. 7, the following characteristic scales are found.

$$\begin{aligned} \text{Length scale : } h_c &= C_w u_*^3 / C_b a g k \Delta T_e \\ \text{Time scale : } t_c &= 1/\omega \\ \text{Temperature scale : } T_c &= \omega C_w u_*^3 / C_b a g k^2 \end{aligned} \quad (12)$$

Governing equations are normalized in terms of these characteristic scales as follows ("~" is capped on each normalized variables).

(a) Heat conservation equation, Eq. 7 :

The surface heat flux,  $F(t)$ , is normalized as

$$\begin{aligned} \tilde{F}(t) &= F(t) / \omega h_c T_c \\ &= -(k/\omega h_c) (\tilde{T}_e - \tilde{T}_m) = -\Delta \tilde{T}_e [\Delta \tilde{T}_e \{\sin(\tilde{t} - \phi) + \sin \phi\} - \tilde{T}_m] \end{aligned} \quad (13)$$

Then, normalized heat conservation relationship is given by

$$d\tilde{S}/d\tilde{t} = -\tilde{F}(\tilde{t}) \quad (14)$$

or

$$\begin{aligned} \tilde{S} &= S / (T_c h_c) = \frac{1}{T_c h_c} \int_0^H T(z) dz = \int_0^{\tilde{H}} \tilde{T}(\tilde{z}) d\tilde{z} = \tilde{T}_m \tilde{h}_m + \int_{\tilde{h}_m}^{\tilde{H}} \tilde{T}_i(\tilde{z}) d\tilde{z} \\ &= \int_0^{\tilde{t}} -\tilde{F}(\tilde{t}) d\tilde{t} \end{aligned} \quad (15)$$

(b) Entrainment relationship :

Eq. 4 :

$$\frac{d\tilde{h}_m}{d\tilde{t}} = \frac{C_b \Delta \tilde{T}_e^2}{\Delta \tilde{T} \tilde{h}_m} [1 - \tilde{h}_m \{\sin(\tilde{t} - \phi) + \sin \phi - \frac{\tilde{T}_m}{\Delta \tilde{T}_e}\}] \quad (16)$$

Eq. 5 :

$$\frac{d\tilde{h}_m}{d\tilde{t}} = \frac{C_b \Delta \tilde{T}_e^2}{\Delta \tilde{T} \tilde{h}_m} [1 - \frac{C_t}{C_b} \tilde{h}_m \{\sin(\tilde{t} - \phi) + \sin \phi - \frac{\tilde{T}_m}{\Delta \tilde{T}_e}\}] \quad (17)$$

In these equations, the dimensionless variables are defined as

$$\begin{aligned} (\tilde{T}_m, \Delta \tilde{T}, \tilde{T}(\tilde{z}), \tilde{T}_i(\tilde{z}), \tilde{T}_e, \tilde{T}_{ea}, \Delta \tilde{T}_e) \\ = (T_m, \Delta T, T(z), T_i(z), T_e, T_{ea}, \Delta T_e) / T_c \end{aligned} \quad (18)$$

$$(\tilde{z}, \tilde{H}, \tilde{h}_m) = (z, H, h_m) / h_c \quad \text{and} \quad \tilde{t} = \omega t \quad (19)$$

#### Dimensionless Governing Parameters

As seen in the normalized equations, Eqs. 15 to 17, the solutions for  $(\tilde{h}_m(\tilde{t}), \tilde{T}_m(\tilde{t}), \tilde{T}_i(\tilde{z}), \tilde{F}(\tilde{t}))$  are governed by the following two parameters.

$$\Delta \tilde{T}_e = \Delta T_e / T_c = (C_b a g k^2 \Delta T_e) / (\omega C_w u_*^3) \quad (20)$$

$$\tilde{H} = H / h_c = (C_b a g k \Delta T_e H) / (C_w u_*^3) \quad (21)$$

$\Delta \tilde{T}_e$  denotes the ratio of surface heat flux magnitude to mechanical turbulence intensity. With increasing  $\Delta \tilde{T}_e$ , surface heat exchange becomes more dominant on thermo-dynamic processes than wind shear stress.

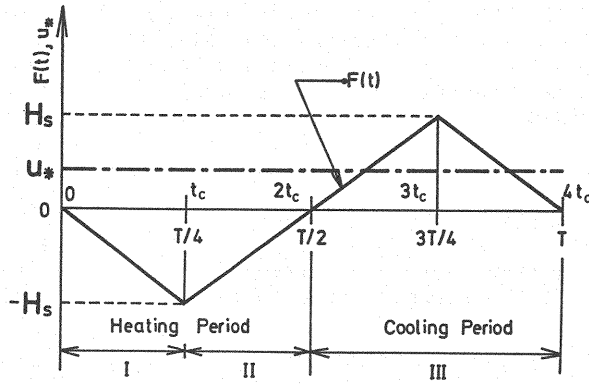


Fig. 4 Time dependency of surface heat flux assumed in the author's previous analysis (Ref.(2))

$\tilde{H}$  is a dimensionless depth denoting the ratio of depth scale to mechanical energy flux. Larger values of  $\tilde{H}$  means "thermo-dynamically deeper lakes".

These two dimensionless parameters are composed of the three independent factors, i.e., (a) thermal meteorological factor,  $\Delta T_e$ , (b) mechanical stirring intensity,  $u_*$ , and (c) depth scale  $H$ .

#### TEMPERATURE ANALYSIS

##### Analysis for Infinitely Deep System

In our previous study (2), infinitely deep water bodies were considered. Seasonal variation of heat flux was assumed as a saw-tooth function as reproduced in Fig. 4. In order to compare the present analysis with the previous one, a computation for the case of  $H \rightarrow \infty$  is carried out.

In Ref.(2), variables were normalized as follows.

$$\begin{aligned} (h_m, z_+) &= (h_m, z)/h_c' \\ (T_m, T_i(z_+), \Delta T_+) &= (T_m, T_i(z), \Delta T)/T_c' \\ t_+ &= t/t_c' \\ F_+(t_+) &= F(t)/H_s \end{aligned} \quad (22)$$

where, subscript "+" denotes normalized variables used in the author's previous paper. The characteristic scales in Eq. 22 are chosen to be  $t_c' = 365/4$  (day),  $h_c' = C_w u_*^3 / C_b \alpha g H_s$ , and  $T_c' = H_s t_c' / h_c'$ , respectively.  $H_s$  is the magnitude of peak surface heat flux (see Fig. 4).

These variables are transformed into the present dimensionless system as follows.

$$\left. \begin{aligned} (\tilde{h}_m, \tilde{z}) &= (k \Delta T_e / H_s) (h_m, z_+) = (\Delta \tilde{T}_e^2 / \tilde{H}_s) (\tilde{h}_m, \tilde{z}_+) \\ (\tilde{T}_m, \tilde{T}_i(\tilde{z}), \Delta \tilde{T}) &= \{ (C_b \alpha g H_s k)^2 \pi / (2 \omega^2 C_w^2 u_*^6) \} (T_m, T_i(z_+), \Delta T_+) \\ &= (\tilde{H}_s^2 / \Delta \tilde{T}_e^2) (\pi/2) (T_m, T_i(z_+), \Delta T_+) \\ \tilde{t} &= (\pi/2) t_+ \\ \tilde{F}(\tilde{t}) &= [ \{ C_b^2 (\alpha g)^2 k^3 \Delta T_e H_s \} / (\omega^2 C_w^2 u_*^6) ] F_+(t_+) = \tilde{H}_s F_+(t_+) \end{aligned} \right\} \quad (23)$$

where,  $\tilde{H}_s = H_s t_c / h_c T_c$  is a dimensionless form of  $H_s$  based on the present system.

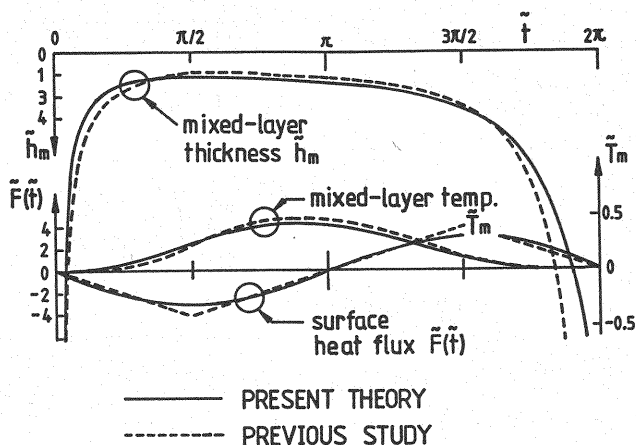


Fig. 5 Comparison of solutions for mixed-layer thickness, mixed-layer temperature and surface heat flux with the previous analytical results. The system is an infinitely deep water body such as ocean (Solid lines: the present analysis, Chain lines: the previous analysis)

The heat flux scale  $\tilde{H}_s$  is determined to be  $\tilde{H}_s=0.4$  for which computed heat flux gives the best fitting to heat flux curve shown in Fig. 4. The result is shown in Fig. 5. Computed mixed-layer thickness  $\tilde{h}_m$  as well as surface temperature  $\tilde{T}_m$  shows good agreement with the former solutions (chain lines in Fig. 5). It confirms that the present analysis gives a reasonable solution without specifying a functional form of heat flux. This is more advantageous than the previous analysis.

#### Comparison with Field Measurements

In order to verify the present analysis, case studies for several lakes are performed. Since our analysis is restricted to lakes located in temperature zones, extreme meteorological conditions are not considered here. In this zone,  $\Delta T_s$  and  $k$  do not vary much and they are assumed to be constant. Based on studies by Mihara et al. (6), they are determined to be  $\Delta T_s=12(^{\circ}\text{C})$ ,  $k=45(\text{cm/day})$ , respectively. Details are shown in Appendix.

On the other hand, there is little available information on  $u_*$  which is friction velocity scale equivalent to annual mean of wind stirring. Generally,  $u_*$  depends not only on local wind velocity but also on horizontal dimensions of lakes and geographical features of surrounding areas. In addition, it is quite difficult to determine a reasonable value for  $u_*$  from wind velocity time series because its time dependent behaviors are irregular and intermittent. In this computation,  $u_*$  is estimated so that computed heat content shows best agreement with the observed one.

Computed heat fluxes and thermal structure development are compared with field measurements for several lakes in Figs. 6 to 9. These data are referred to Refs.(7) to (9). In these figures, the agreement between the theory and field data is satisfactory. In addition,  $u_*$  determined by the present method shows reasonable values for all lakes. We conclude that the proposed analysis can reproduce temperature fields with satisfactory agreement, although some of processes are roughly formulated.

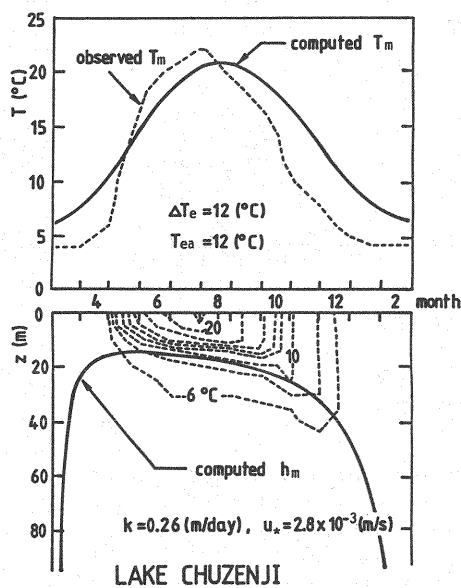


Fig. 6 Comparison between the theory and field data in Lake Chuzenji (8)

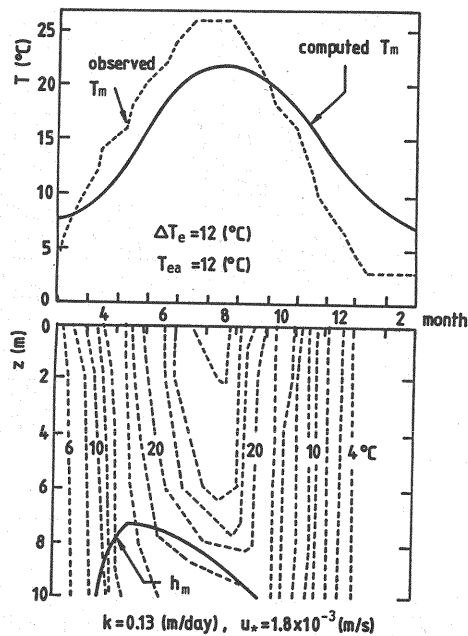


Fig. 7 Comparison between the theory and field data in Lake Kawaguchi (7)

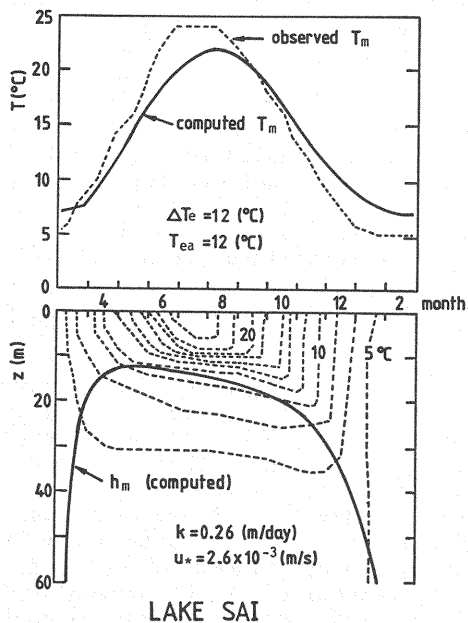


Fig. 8 Comparison between the theory and field data in Lake Sai (7)

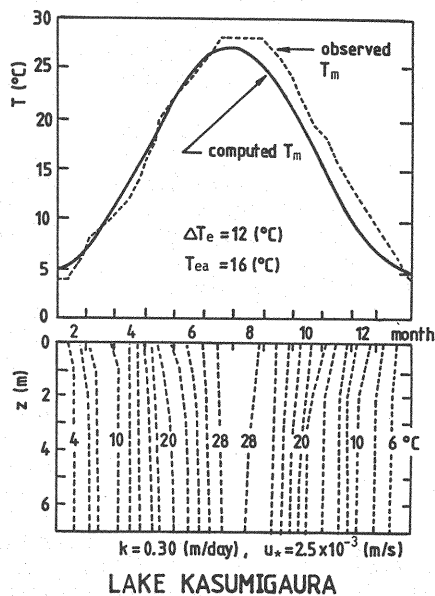


Fig. 9 Comparison between the theory and field data in Lake Kasumigaura (9)

# CLASSIFICATION OF LAKES THERMAL STRUCTURE

## Sensitivity of Thermal Processes to Governing Parameters

A parametric analysis is carried out to examine sensitivity of the solutions of temperature and heat flux to the two governing parameters,  $\Delta T_0$  and  $\tilde{H}$ . Some results for different combinations of  $(\tilde{H}, \Delta T_0)$  are exemplified in Fig. 10. Temperature isopleths are shown in depth-time coordinates in the upper parts of every diagrams. The corresponding time development of heat flux,  $\tilde{F}(\tilde{t})$ , and mixed-layer temperature,  $\tilde{T}_m$ , are shown in the lower parts. Since temperature field in the lower layer of stratification is assumed to be unchanged, every temperature contour lines below the thermocline are kept horizontal. In a real situation, however, the temperature slightly changes even in this region.

The following conclusions can be drawn from the figure.

- a) Larger the depth scale  $\tilde{H}$ , stronger the temperature stratification becomes, i.e., life span of thermocline becomes longer with increasing  $\tilde{H}$ .
- b) With increasing  $\Delta T_0$ , seasonal variation of surface heat flux and surface water temperature becomes larger.
- c) Three types of thermal structure behaviors are found;
  - (A) Completely mixed type lake [M-type]  
No thermal stratification is found throughout a year.
  - (B) Partially mixed type lake [MS-type]  
Weak stratification develops in the beginning of heating period. But it is destroyed by wind stirring after decrease in the heating rate. The system is completely overturned before cooling season begins.
  - (C) Stratified type lake [S-type]  
Strong thermal stratification develops, which is kept throughout the heating period. Then, in the cooling season, it begins to be destroyed under the combined action of thermal convection and mechanical turbulence. Finally, the system is uniformly mixed.

## Hysteresis of Heat Content, Surface Temperature and Potential Energy

Time hystereses of "S- $T_m$ " and " $T_m$ -P" are useful for understanding relative phase relationships among these quantities. They are also useful to examine how accurately the theoretical model reproduces seasonal variations of thermo-dynamic properties (10).

In the normalized system,  $\tilde{S}$  and  $\tilde{T}_m$  are defined by Eqs. 15 and 18, respectively. Dimensionless potential energy  $\tilde{P}$  of water column are given as

$$\tilde{P} = \frac{1}{2} \tilde{T}_m \tilde{h}_m^2 + \int_{h_m}^{\tilde{H}} \tilde{T}_i(z) \tilde{z} d\tilde{z} \quad (24)$$

where the potential energy is taken to be deviation from the initial value. Its dimensional form is written as

$$P = \int_0^H \rho_0 \alpha g T(z) z dz \quad (25)$$

The potential energy is composed of two components. The first one is "Dynamic Potential Energy",  $P_1$ , which reflects dynamic stability of buoyancy stratification. This is equivalent to energy being necessary to completely destroy stratification through adiabatic process, in other words, work done by full-scale mixing. For uniform temperature field,  $P_1$  is zero. The second component is "Thermal (or Internal) Potential Energy",  $P_2$ , which is the contribution of heat energy in water column to the potential energy. This component has no effect on dynamic process.

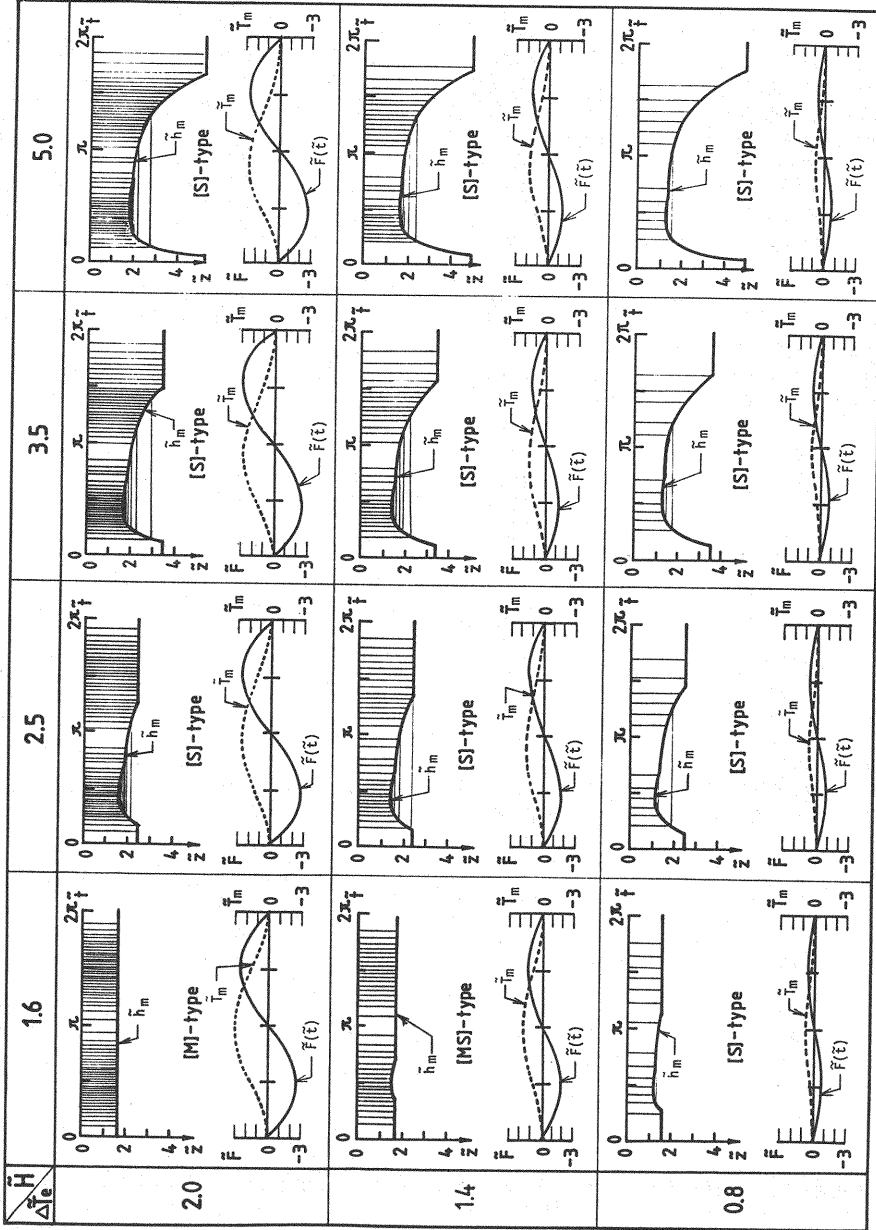


Fig. 10 Computed seasonal variations of temperature fields and surface heat flux for different combinations of  $(\Delta T_e, H)$ . The upper parts show computed temperature isopleths. The lower parts represent surface heat flux,  $\tilde{F}(\tilde{t})$ , in solid curves and surface water temperature,  $\tilde{T}_m$ , in broken lines, respectively.

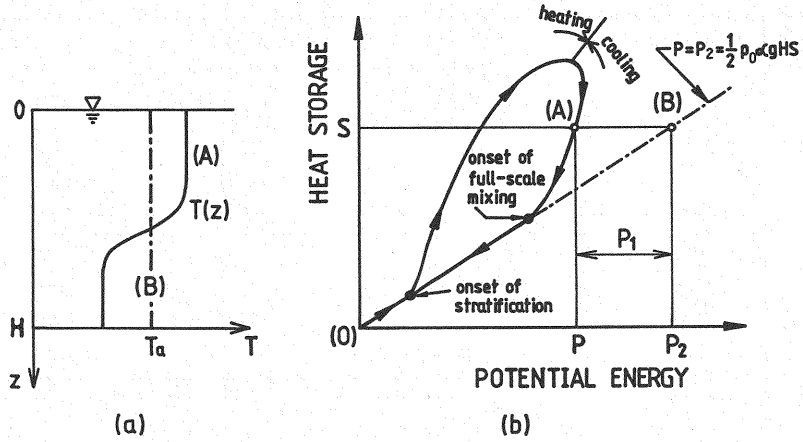


Fig. 11 (a) Two kinds of temperature field,  
 (A) stratified system  
 (B) corresponding completely mixed situation  
 produced by adiabatic vertical mixing  
 (b) A schematic diagram of the \$(S-P)\$ hysteresis  
 loop and relationship among \$P\$, \$P\_1\$, \$P\_2\$ and \$S\$  
 in the \$(S-P)\$ plane

For better our understanding of physical meanings for \$P\$, \$P\_1\$ and \$P\_2\$, two regimes of temperature fields are schematically shown in Fig. 11(a). Consider the two situations; (A): stratified system and (B): uniformly mixed system whose heat storage is equal to (A). \$P\$ corresponds to (A) and \$P\_2\$ to (B), respectively. Thus, \$P\_2\$ is defined as

$$P_2 = \int_0^H \rho_0 g T_a z dz = \frac{1}{2} \rho_0 g T_a H^2 = \frac{1}{2} \rho_0 g H S \quad (26)$$

where \$T\_a\$ is ensemble mean temperature defined by \$T\_a = S/H\$.

The potential energy difference between these two situations, say \$(P\_2 - P)\$, is equal to the work done by vertical mixing. We define it to be the dynamic potential energy as

$$P_1 = P_2 - P = \int_0^H \rho_0 g T(z) (z - \frac{H}{2}) dz \quad (27)$$

\$P\_2\$ reflects the thermal energy transfer process and \$P\_1\$ the dynamic energy transfer process, respectively. Dimensionless forms for \$P\_1\$ and \$P\_2\$ are written as follows, respectively.

$$\tilde{P}_1 = \int_0^{\tilde{H}} \tilde{T}(\tilde{z}) (\tilde{z} - \frac{\tilde{H}}{2}) d\tilde{z}, \quad \tilde{P}_2 = \frac{1}{2} \tilde{T}_a \tilde{H}^2 = \frac{1}{2} \tilde{S} \tilde{H} \quad (28)$$

Definition of \$P\$, \$P\_1\$ and \$P\_2\$ are schematically shown in a hysteresis loop diagram of \$(S-P)\$ in Fig. 11(b).

Sensitivity of hysteresis loops of \$(\tilde{T}\_m - \tilde{S})\$, \$(\tilde{P} - \tilde{S})\$ and \$(\tilde{P}\_1 - \tilde{S})\$ to the two parameters \$\tilde{H}\$ and \$\Delta \tilde{T}\_e\$ are seen in Fig. 12. The hystereses of \$(\tilde{P}\_2 - \tilde{S})\$ are not shown, because they have no loop; \$\tilde{P}\_2\$ is just in proportion to \$\tilde{S}\$ as seen in Eq. 28-2. In the \$(\tilde{T}\_m - \tilde{S})\$ diagrams, it can be seen that relative phase lag between \$\tilde{T}\_m\$ and \$\tilde{S}\$ becomes larger with increasing \$\tilde{H}\$ but it is not so sensitive to \$\Delta \tilde{T}\_e\$. A similar tendency is seen in the relationships between \$\tilde{P}\$ and \$\tilde{S}\$. The

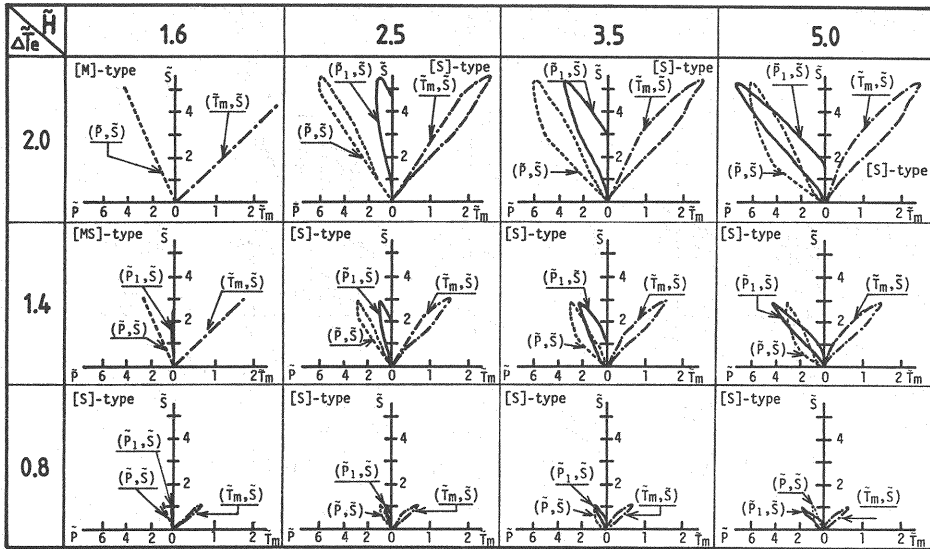


Fig. 12 Time hysteresis loops of  $\tilde{S}-\tilde{T}_m$  (right hand side),  $\tilde{P}-\tilde{S}$  (thin solid lines in the left hand side) and  $\tilde{P}_1-\tilde{S}$  (thick solid lines in the left hand side) for various combinations of  $(\tilde{H}, \Delta \tilde{T}_e)$

loop curves of  $(\tilde{T}_m-\tilde{S})$  and  $(\tilde{P}-\tilde{S})$  for the case of large  $\tilde{H}$  are qualitatively in good agreement with the results of Gill and Turner (10) which were obtained for infinitely deep water bodies.

We postulate that the conventional potential energy  $\tilde{P}$  is not an appropriate index for examining dynamic aspects of temperature field because it includes the component due to heat storage,  $\tilde{P}_2$ , in addition to the dynamic component,  $\tilde{P}_1$ .  $\tilde{P}_2$  is determined solely by heat storage. This is independent on temperature profiles, in other words, independent on dynamic energy transfer process due to stratification and destratification. On the other hand,  $\tilde{P}_1$  is physically more meaningful in the examination of dynamic energy transfer process from external systems into lakes. The hystereses of  $(\tilde{P}_1-\tilde{S})$  are shown in thick solid curves in Fig. 12. In better mixed situations such as M-type or MS-type lakes, less dynamic potential energy  $\tilde{P}_1$  is stored. For thermo-dynamically deeper lakes, in other words, for lakes of larger depth scale  $\tilde{H}$ , more amount of  $\tilde{P}_1$  is stored and the stratification system is gravitationally more stable.  $\tilde{P}_1$  becomes zero when the system is completely mixed, which means that no dynamic energy is stored and the system is gravitationally neutral. Although the conventional potential energy  $\tilde{P}$  cannot describe these dynamic behaviors, the proposed dynamic potential energy  $\tilde{P}_1$  well documents the thermo-dynamic aspects of lakes.

#### Classification of Lake Thermal Structure

A parametric analysis with respect to the two parameters,  $(\tilde{H}, \Delta \tilde{T}_e)$ , leads to a classification diagram of lake thermal structure as shown in Fig. 13, where the three types of annual thermal structures are shown in the  $(\tilde{H}, \Delta \tilde{T}_e)$  coordinate system. Thin solid curves in the figure denote contour curves of the "thermocline life span" during which thermocline exists. Numerical values are dimensionless life span of thermocline which are in the range of

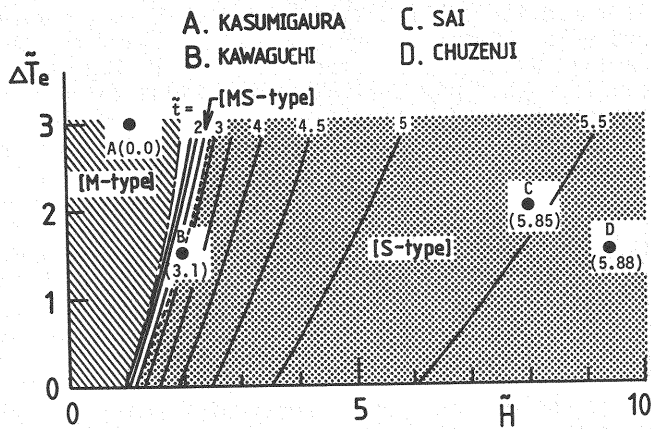


Fig. 13 Classification diagram of lake thermal structure (thin solid lines show contour curves of thermocline life span)

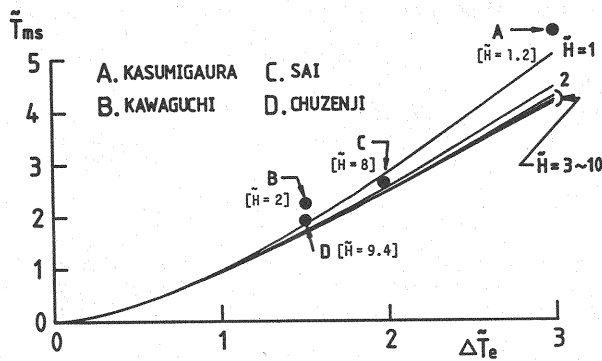


Fig. 14 Functional dependency of maximum surface temperature,  $\tilde{T}_{ms}$ , on  $\Delta \tilde{T}_e$  and  $\tilde{H}$ .

$0 \leq \tilde{t} \leq 2\pi$ . Also shown in black circles are field data from several lakes, where numerical values correspond to observed thermocline life span.

In Fig. 14, the maximum surface water temperature in a year,  $\tilde{T}_{ms}$ , is shown as a function of  $\Delta \tilde{T}_e$  and  $\tilde{H}$ .

In both Figs. 13 and 14, agreement between the analysis and field data is satisfactory. Fig. 13 shows that thermocline life span is more sensitive to  $\tilde{H}$  than to  $\Delta \tilde{T}_e$ . On the other hand, in Fig. 14, it is seen that  $\tilde{T}_{ms}$  is more dominantly affected by the amplitude of equilibrium temperature,  $\Delta \tilde{T}_e$ , than by  $\tilde{H}$ .

From the results, it is concluded that the proposed analysis is practically useful to classify lakes from a thermo-dynamic point of view. It also enables us to examine lake properties without requiring detail in-situ meteorological data.

#### CONCLUDING REMARKS

We examine how thermal structure and heat flux in lakes are affected by relating factors. The heat flux formula using an equilibrium temperature has an advantage that we need not specify a time-dependent functional form of heat

flux. The seasonal variation of heat flux is given as a solution of the lake temperature analysis. Satisfactory agreement between the theory and field data is recognized not only in temperature field but also in surface heat flux, which confirms that our analysis has satisfactory resolution for reproducing annual thermal processes.

Based on the model, we obtain two dimensionless governing parameters; they are (a) dimensionless amplitude of an equilibrium temperature,  $\Delta\tilde{T}_e$ , and (b) dimensionless depth of water body,  $\tilde{H}$ . From a thermo-dynamic point of view, lakes are classified into three categories; they are (a) mixed type lake, (b) partially mixed type lake and (c) stratified type lake. We proposed a classification diagram, where the three categories as well as thermocline life span are shown as functions of  $\Delta\tilde{T}_e$  and  $\tilde{H}$ . The present analysis enables estimation of thermal regimes of lakes without specifying meteorology and heat exchange processes.

We hope that this research work could contribute to, for instance, a preliminary investigations of water resources development project, improvement and protection works of hydrospheric environment and so on.

In lakes, however, there must be some additional important processes not included in the present analysis, such as horizontal heat advection of through-flows, wind-induced currents, temperature stratification below 4°C, ice formation, etc.. It is necessary to extend the analysis to more realistic situations by examining these processes.

#### ACKNOWLEDGEMENTS

The authors are grateful to Prof.Yano and Prof.Kanda, Kobe University and Prof.Murota, Osaka Industrial University for their excellent supervision in performing this study.

#### REFERENCES

1. Tetzlaff, G. : The daily cycle of the water temperature of a shallow lake, Developments in Water Science, 11, Hydrodynamics of Lakes, edited by Graf, W.H. and Mortimer, C.H., Elsevier, pp.325-330, 1979.
2. Michioku, K., A.Murota and S.Sakaguchi : Seasonal thermal cycle in stratified deep lakes, J.Hydroscience and Hydraulic Engineering, Vol.9, No.1, pp.11-26, 1991.
3. Murota, A., K.Michioku : Dynamic effect of stabilizing buoyancy flux upon entrainment induced by oscillating-grid turbulence, Proceedings of Asian and Pacific Regional Division of IAHR, pp.117-184, 1988.
4. Murota, A. and K.Michioku : Vertical mixing process in thermally stratified system induced by combined action of mechanical and thermal stirring, Proceedings of Asian and Pacific Regional Division of IAHR, pp.183-202, 1986.
5. Kraus, E.B. and J.S.Turner : A one-dimensional model of the seasonal thermocline, II. The general theory and its consequences, Tellus, 19, pp.98-105, 1967.
6. Mihara, Y., Uchijima, Z., Nakamura, S. and Onuma, K. : A study on heat balance and water temperature rising of the warming pond, Bulletin of the National Institute of Agricultural Sciences, A-7, pp.1-43, 1959 (in Japanese).
7. Arai, T. and T.Nishizawa : Theory of water temperature (Suion-ron), pp.44-46, Kyoritsu Press, 1974 (in Japanese).
8. Muraoka, K. and T.Hirata : Thermal stratification and internal wave in Lake

Chuzenji, Research Report from the National Institute for Environmental Studies, 69, pp.5-35, 1984 (in Japanese).

9. Goda, T. : Limnological data in Kasumigaura, Research Report from the National Institute for Environmental Studies, No.6, pp.335-403, 1979 (in Japanese).
10. Gill, A.E. and J.S. Turner : A comparison of seasonal thermocline models with observation, Deep-Sea Research, Vol.23, pp.391-401, 1976.

## APPENDIX

### Appendix-1 $k$ : HEAT EXCHANGE COEFFICIENT

Numerical value of  $k$  is uncertain. Strictly speaking, it is not constant, and might weakly depend on meteorological conditions such as horizontal fetch of lakes, geography of surrounded area and so on. In the present study, however,  $k$  is approximated to be constant and estimated as follows.

The following two proposals were given for  $h$  and  $S$ .

- (a) Mihara et al. (6);

$$h=17.0 \text{ (cal/cm}^2\text{day}^\circ\text{C)} \text{ or } h=2.0 \times 10^{-4} \text{ (cal/cm}^2\text{sec}^\circ\text{C)} \quad (\text{A.1})$$

$$S=34.5 \text{ (cal/cm}^2\text{daymmHg)} \text{ or } S=4.0 \times 10^{-4} \text{ (cal/cm}^2\text{secmmHg)} \quad (\text{A.2})$$

These are obtained from field data in small impoundments whose horizontal dimensions are less than 100(m).

- (b) Timofeev proposal (see Ref.(6));

$$h=4.8(U_2/x^{0.1}) \text{ (cal/cm}^2\text{day}^\circ\text{C)} \quad (\text{A.3})$$

$$S=11.6(U_2/x^{0.1}) \text{ (cal/cm}^2\text{daymmHg)} \quad (\text{A.4})$$

where,  $U_2$  : wind velocity at 2(m) above the water surface (m/sec) and  $x$  : fetch (m). These formulas are for larger water areas with horizontal scales of  $1(\text{km}) \leq x \leq 100(\text{km})$ . Taking  $U_2=2(\text{m/s})$  and  $x=1000(\text{m})$  for an example, Eqs. A.3 and A.4 reduce to

$$h=4.8 \text{ (cal/cm}^2\text{day}^\circ\text{C)} \quad (\text{A.5})$$

$$S=11.6 \text{ (cal/cm}^2\text{daymmHg)} \quad (\text{A.6})$$

$\beta$  varies between  $0.5(\text{mmHg}/^\circ\text{C}) \sim 2.2(\text{mmHg}/^\circ\text{C})$  for normal water temperature condition and we take  $\beta=1.2(\text{mmHg}/^\circ\text{C})$ . Then, Eqs. A.1 and A.2 give

$$K=68 \text{ (cal/cm}^2\text{day}^\circ\text{C)} \text{ or } k=K/\rho c=68 \text{ (cm/day)} \quad (\text{A.7})$$

and Eqs. A.5 and A.6 give

$$K=24 \text{ (cal/cm}^2\text{day}^\circ\text{C)} \text{ or } k=K/\rho c=24 \text{ (cm/day)} \quad (\text{A.8})$$

Taking the ensemble mean of Eqs. A.7 and A.8, we used

$$k=45 \text{ (cm/day)}.$$

### Appendix-2 $\Delta T_e$ : MAGNITUDE OF EQUILIBRIUM TEMPERATURE VARIATION

Based on data given by Uchijima (7), we take  $\Delta T_e=12(^\circ\text{C})$ .

### Appendix-3 $u_*$ : FRICTION VELOCITY

Considering that  $u_*$  varies between  $0.1 \sim 0.8(\text{cm/s})$ , we use  $u_*=0.4(\text{cm/s})$  for the parametric analysis.

### Appendix-4 NOTATION

The following symbols are used in this paper.

$c$	= specific heat of water;
$C_w, C_b, C_f$	= proportional coefficients in entrainment relationships;
$h_c$	= characteristic scale of depth;
$h_m$	= mixed-layer thickness;
$F(t)$	= heat flux per horizontal unit area at water surface;

$g$	= gravity acceleration;
$H$	= total depth of water body;
$k(=K/\rho c)$ , $K$	= heat exchange coefficients at water surface;
$P$ , $P_1$ and $P_2$	= conventional potential energy, dynamic potential energy and thermal potential energy in density stratification system, respectively;
$S$	= heat storage of water column with unit horizontal area;
$t$	= time coordinate;
$t_0$	= characteristic scale of time;
$T_0$	= characteristic scale of temperature;
$T_e$	= equilibrium temperature;
$T_l(z)$	= water temperature at lower stratified layer;
$T_m$	= water temperature in the mixed-layer;
$\Delta T$	= temperature jump at thermocline interface;
$\Delta T_e$ , $T_{ea}$	= amplitude and average in seasonal variation of equilibrium temperature, respectively;
$u_b$	= velocity scale for heating buoyancy flux;
$u_f$	= velocity scale for natural convection;
$u_*$	= friction velocity of wind shear stress at water surface;
$z$	= vertical coordinate measured downwards from water surface;
$\alpha$	= coefficient of thermal expansion;
$\epsilon = \alpha \Delta T$	= specific density differences of temperature jump, $\Delta T$ , at thermocline interface;
$\phi$	= phase lag in sinusoidal variation curve of equilibrium temperature;
$\rho$	= density of water;
$\omega = 2\pi/365$	= angular frequency;

(Received March 11, 1991; revised January 27, 1992)